Characterization of biogenic ferrihydrite nanoparticles by means of SAXS, SRD and IBA methods

IOP Conf. Series: Journal of Physics: Conf. Series **994** (2018) 012012 doi:10.1088/1742-6596/994/1/012012

Characterization of biogenic ferrihydrite nanoparticles by means of SAXS, SRD and IBA methods

M Balasoiu[1,2*], S Kichanov[1], A Pantelica[2], D Pantelica[2], S Stolyar[3,4], R Iskhakov[4], D Aranghel[1, 5], P Ionescu[2], C R Badita[2], S Kurkin[6], O Orelovich[1], S Tiutiunikov[1]

[1] Joint Institute for Nuclear Research, Dubna, 141980 Moscow Region, Russia
[2] Horia Hulubei National Institute for Physics and Nuclear Engineering, Bucharest, Romania
[3] Siberian Federal University, 660041, Krasnoyarsk, Russia
[4] Kirensky Institute of Physics, Siberian Branch of RAS, 660036, Krasnoyarsk, Russia
[5] Extreme Light Intrastructure Nuclear Physics (ELI-NP), Bucharest, Romania
[6] Institute of Synthetic Polymer Materials RAS, Moscow, 117393, Russia

balas@jinr.ru

Abstract. Investigations of biogenic ferrihydrite nanoparticles produced by bacteria *Klebsiella oxytoca* by applying small angle X-ray scattering, synchrotron radiation diffraction and ion beam analysis methods are reviewed. Different experimental data processing methods are used and analyzed.

1. Introduction

A large number of microorganisms produce inorganic nanostructures with controlled size, shape, composition and other properties similar to chemically synthesized materials [1, 2].

In the present work, investigations of biogenic ferrihydrite nanoparticles produced by bacteria *Klebsiella Oxytoca* by applying small angle X-ray scattering (SAXS), synchrotron radiation diffraction (SRD) and ion beam analysis (IBA) methods are reviewed. SAXS enables to measure structural features on length scales between 1 nm up to several hundred of nanometers by analyzing the scattering pattern at very low angles from the direct X-ray beam. By examining X-rays that are scattered at small angles to the primary X-ray beam, it can be obtained information that is directly proportional to the size and shape of nanometer-sized objects [3]. Synchrotron radiation sources (SRS) have several advantages over conventional X-radiation sources, including a wider spectrum and higher luminosity, which allows one to reduce essentially the time of conventional X-ray experiments. The IBA techniques with multi-elemental capabilities, high sensitivity and low detection limits offer perfect methods for elemental characterization of materials [4]. In particular, the simultaneous application of particle-induced X-ray emission (PIXE), particle-induced gamma-emission (PIGE) and Rutherford backscattering spectrometry (RBS) with proton beam can provide quantitative elemental information on a broad range of chemical elements.

2. Experimental

2.1. Biogenic ferrihydrite samples

The investigated samples are ferrihydrite nanoparticles produced by bacteria *Klebsiella Oxytoca* in the course of biomineralization of iron salt solutions from natural environment [5-7]. The bacterial biomass isolated from the sapropel obtained from the Lake Borovoe (Krasnoyarsk region) was grown under microaerophilic conditions on a Lovley medium of composition (g/L) NaHCO3, 2.5; CaCl2·H2O, 0.1; KCl, 0.1; NH4Cl, 1.5; and NaH2PO4·H2O, 0.6. The ferric citrate concentration was varied from 0.2 to 5 g/L, the yeast extract concentration was 0.05 g/L, and the benzoic acid concentration was varied from 0.2 to 0.5 g/L.

As a result of variation of the growth conditions for the microorganisms (growth period, light exposition, potassium citrate – ferric citrate rate, etc.), bacterium *Klebsiella oxytoca* creates, as was established in previous works [6-11] different types of ferrihydrite nanoparticles. Two types of ferrihydrite nanoparticles (Fe12 and Fe34), separated from a bacterial biomass grown during 8 and 21 days, respectively, were accurately identified by means of Mossbauer spectroscopy [7] and static magnetic measurements analysis [8].

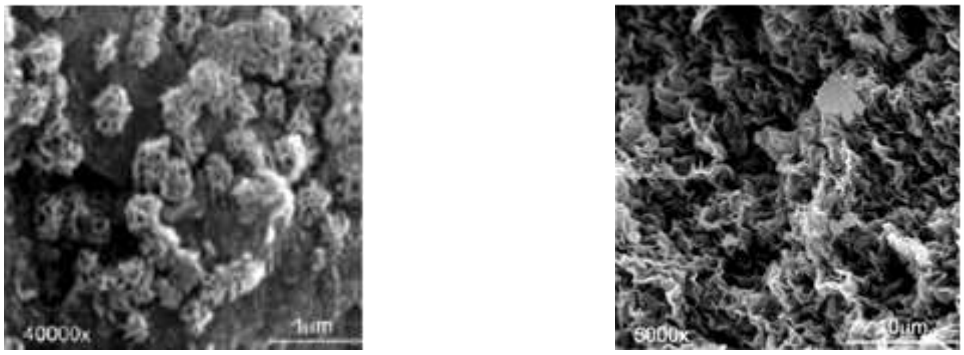

(a) (b)

Fig.1 SEM images of two dry samples containing ferrihydrite nanoparticles obtained from a bacterial biomass grown during 8 and 21 days, respectively; sample Fe12 (a) and sample Fe34 (b).

Earlier studies [1, 11] of the morphology and structure investigation of these two ferrihydrite samples produced by *Klebsiella Oxytoca* by means of a number of procedures at different length scales: optical microscopy; scanning electron microscopy (Figs.1 a, b), transmission electron microscopy and small angle X-ray scattering have given the results presented in [1-2, 12].

Spectroscopic studies (absorption, fluorescence emission, and FT-IR) [12-14] confirmed the presence of polysaccharides but also of some traces of proteins.

The preliminary determination of the elemental composition of a ferrihydrite sample grown during 2 weeks was accomplished using X-ray fluorescence analysis (XRF) (see Table 1) [12].

Table 1 Elemental contents determined by XRF in the Fe12 biogenic ferrihydrite sample, in percent d.w. (dry weight) [12]

Element	Fe12
O	60.53
C	16.51
P	8.45
Fe	9.20
Ca	2.93
K	1.68
Cl	0.33
Other elements	0.38

In order to characterize the samples with improved analytical sensitivity, also for an analytical quality control, a combined use of different techniques is often required. Within this context, a combined use of PIXE, PIGE, and RBS with 3 MeV proton beam was simultaneously accomplished.

2.2. Small angle X-ray scattering

Small angle X-ray scattering data were obtained at Brucker Nanostar SAXS spectrometer at the Institute of Synthetic Polymer Materials RAS, Moscow. The X-ray scattering intensity is experimentally determined as a function of the scattering vector Q whose modulus is given by $Q = (4\pi/\lambda)\sin\theta/2$, where λ is the X-ray wavelength, and θ is the scattering angle between the directions of the scattered and transmitted beams. The experimental setup used covered the Q range of $0.01 \div 0.11$ Å^{-1}.

2.3. Diffraction experiment at SRS

Synchrotron radiation sources have several advantages over conventional X-radiation sources, including a wider spectrum and higher luminosity. This is the reason why synchrotron radiation has been increasingly used in the world to solve a wide spectrum of fundamental and applied problems in physics, chemistry, materials science, biology, medicine and earth sciences.

The Kurchatov Synchrotron Radiation Source (KSRS) in Moscow is the first Russian source put into operation for investigations at X-ray energies up to 40 keV. One of the stations that have been created at the source is the experimental station “Mediana” [15], which hosts facilities for powder diffractometry, tomography and refraction introscopy. The equipment layout at the “Mediana” station is shown in Fig.2.

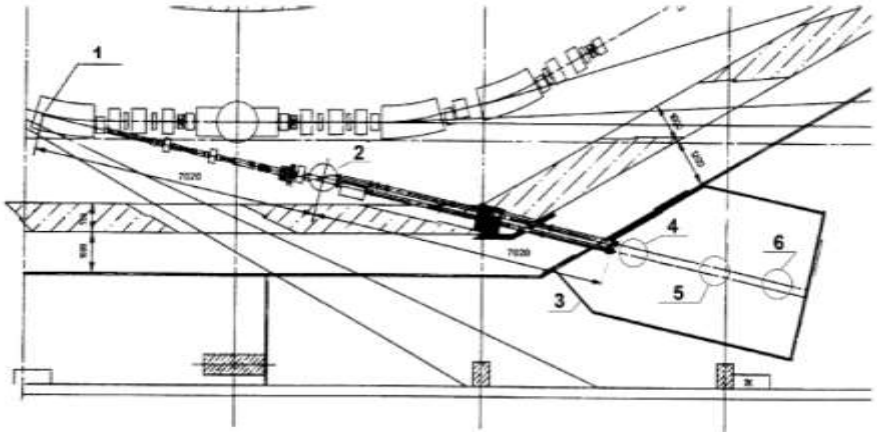

Fig. 2 Layout of the “Mediana” station: 1, radiation source; 2, monochromators; 3, experimental hutch; 4, position of the diffractometer; 5, position of the tomography unit; 6, position of the introscopy unit [15].

One of the topical problems to be solved with the help of synchrotron radiation is the investigation of the structure and phase diagrams of condensed matter. High intensity of the synchrotron radiation beam allows carrying out experiments with small volumes of the investigated matter.

2.4. Ion beam analysis

The 3 MV Tandetron accelerator installed in 2012 at Tandem Accelerators Department (DAT) of the Horia Hulubei National Institute for Physics and Nuclear Engineering (IFIN-HH) is mainly dedicated to applied physics experiments [16]. The machine is fully equipped for ion beam analysis and ion implantation experiments (Fig. 3).

The first beam-line has specific detectors and electronic systems to perform PIXE, PIGE, RBS, and elastic recoil detection analysis (ERDA) (Fig.4).

IBA provides an excellent way to investigate atomic compositions and concentrations in various materials. IBA techniques are characterized by high precision and reliability. In most cases, before the analysis, the samples do not need any chemical or physical preparation, direct rapid analysis is available under vacuum or outside the reaction chamber, in air or in the atmosphere of He to improve the accuracy of the results. The main advantage of this method is its non-invasive profile, which makes it excellent for biological and brittle specimens.

Fig.3 The 3 MV Tandetron accelerator [16] at Tandem Accelerators Department of IFIN-HH [15].

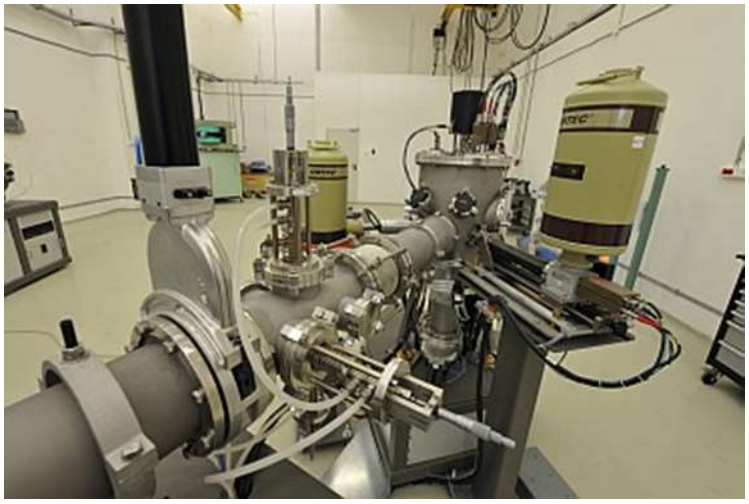

Fig.4 The first beam-line of 3 MV Tandetron accelerator equipped to perform ion beam analysis, e.g. PIXE, PIGE, RBS, and ERDA [16].

3. Results and discussion

3.1. Small angle X-ray scattering

The experimental curve obtained from Sample Fe34 reveals in the q range of 0.01 ÷ 0.11 $Å^{-1}$ a power-law behavior:

$$I(q) \approx q^{-\alpha},$$

with the exponent $\alpha = 3.18 \pm 0.01$. This means that the system has a fractal structure. When $3 < \alpha < 4$, the scattering objects are considered to be surface fractals and the fractal dimension is given by formula $D_S = 6 - \alpha$ [17, 18].

Consequently, for Fe34 sample, the system structure is characterized by a fractal dimension of $D_S = 2.82 \pm 0.01$, which is specific to highly branched surface fractals [9].

For sample Fe12, the experimental curve presents 2 regions with a power-law behavior: 0.01 ÷ 0.022 $Å^{-1}$ and 0.08 ÷ 0.18 $Å^{-1}$. In these cases, the exponent α has the values (i) $\alpha = 2.08 \pm 0.05$ and (ii) $\alpha = 2.86 \pm 0.02$, respectively. For these values, α gives the mass fractal dimension $D_M = \alpha$, characterizing randomly distributed objects as lamellae or platelets (i) [17] and low-dimensional clustering aggregates (ii) [19].

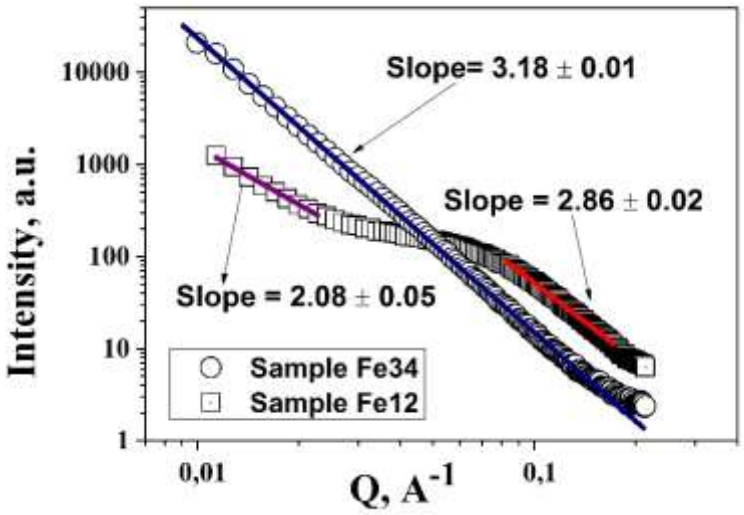

Fig.5 Small angle X-ray scattering experimental curves from dry samples Fe12 (square symbol) and Fe34 (circle symbol) and the power-law fits of the experimental data.

3.2. Diffraction experiment at SRS

The experimental and processed diffraction spectra of biogenic ferrihydrite nanoparticles samples Fe12 and Fe34 obtained at "Mediana" station of the KSRS are given in Fig.6.

The diffraction peaks from the sample are located at scattering angles of $2\theta = 5.4^0$; 8.1^0; 16^0. Besides this, around the scattering angles of $2\theta = 10^0$-13^0 is observed a diffusive halo.

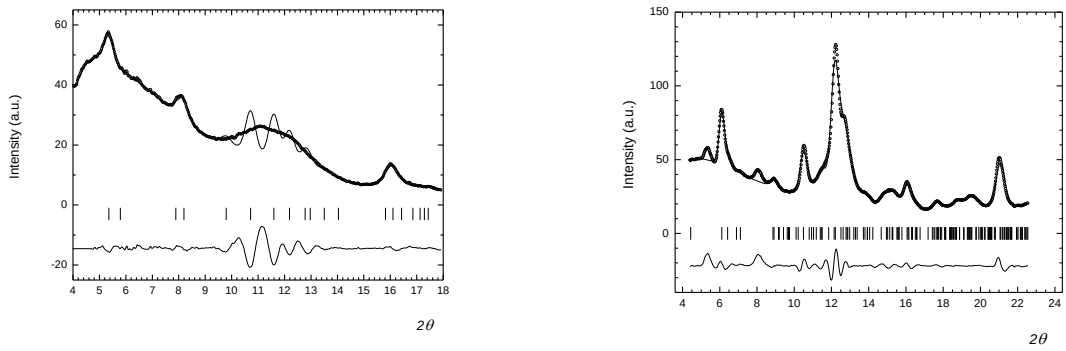

a b

Fig.6 The processing of diffraction spectra sections of: (a) sample Fe12 (using a tetragonal cell model) and (b) of sample Fe34 (using a monoclinic cell) [20].

The processing of a spectrum section of sample Fe12 was accomplished using a tetragonal cell model (a=b=5.81Å, c=6.28 Å). In this case, the peaks located at the scattering angle $2\theta = 5.4^0$; 8.1^0; 16^0 are reflections of the interplanar distances with Miller indices (001) (110) and (003), respectively (see Fig.6 a). In the case of the diffraction spectrum of sample Fe34, a possible description of the structure is the model using a monoclinic cell (a = 3.79, b = 11.04, c = 10.54, β =95.26) (see Fig.6 b). In the diffraction pattern of this sample, one should note the presence of the reflections observed in the spectrum of sample Fe12 at scattering angles $2\theta = 5.4^0$; 8.1^0; 16^0 [20].

3.3. Ion beam analysis

PIXE, PIGE, and RBS complementary ion beam techniques were simultaneously used to provide information on elemental content of biogenic ferrihydrite nanoparticles produced by *Klebsiella Oxytoca* [20].

A total 14 elements were determined by PIXE in the examined samples, as follows (concentration levels in descending order, in parentheses): Fe, P, Cl, Ca, and K (tens of percent to percent); Hg, Pb, Al, Si, Rb, and S (tenths of percent); Rb, S, Zn, Cr, and Mn (hundreds of ppm/ part per million).

PIGE results were obtained for Na, Mg, P, Cl, and Fe (5 elements) in Fe12 and Fe34 samples. Major elements Fe, P, and Cl determined by PIGE were found to be at similar levels with those obtained by PIXE (Table 2). In addition, Na and Mg in Fe12 and Fe34 samples were measured by PIGE at levels of (0.80-0.23) % and (1.82-1.10) %, respectively.

RBS results for P, Cl, K, Ca, and Fe are in agreement with those determined by PIXE and PIGE.

By comparing Fe12 and Fe34 samples, higher contents of Fe, P, Si, Hg, Pb, and Rb in Fe34 (ratios between 1.2 and 3), and higher contents of Ca, K, Mg, Na, and Cl in Fe12 (ratios between 1.2 and 10) were found. The elements Cr, and S in Fe34, and Zn and Mn in Fe12 were also determined.

Concerning the light elements determined by RBS, similar mass fractions for O in both samples, 1.5 times higher content for C in Fe34, as well as 1.2 and 2.4 times higher contents for H and N in Fe12, respectively, were observed.

The discrepancy of the elemental contents between IBA results and earlier results obtained by XRD [12] can be explained first by the fact that samples have been extracted differently from the biomass as previously and secondly by the specificity of the investigation method. The cleaning method was improved in order to succeed to eliminate as much as possible the bacterial residues.

Table 2. Elemental contents (percent d.w.) determined by PIXE, PIGE and RBS in Fe12 and Fe34 biogenic ferrihydrite samples grown during 8 and 21 days, respectively.

Element/ Method	Fe12			Fe34		
	PIXE	PIGE	RBS	PIXE	PIGE	RBS
Na	-	0.804 ± 0.040	-	-	0.234 ± 0.012	-
Mg	-	1.82 ± 0.60	-	-	1.10 ± 0.64	-
H	-	-	3.61	-	-	3.08
C	-	-	8.12	-	-	11.9
N	-	-	5.07	-	-	2.14
O	-	-	35.9	-	-	36.7
Al	0.327 ± 0.007	-	-	0.356 ± 0.009	-	-
Si	0.184 ± 0.008	-	-	0.233 ± 0.013	-	-
P	12.3 ± 0.1	10.5 ± 0.5	6.44	15.1 ± 0.1	11.1 ± 0.6	11.2
S	< 0.02	-	-	0.16 ± 0.02	-	-
Cl	11.9 ± 0.1	7.70 ± 1.00	6.86	1.19 ± 0.01	0.89 ± 0.31	0.92
K	6.44 ± 0.02	-	4.10	4.11 ± 0.01	-	3.08
Ca	7.98 ± 0.03	-	5.29	6.67 ± 0.02	-	5.06
Cr	< 0.01	-	-	0.027 ± 0.01	-	-
Mn	0.094 ± 0.003	-	-	< 0.01	-	-
Fe	27.0 ± 0.1	25.9 ± 1.8	24.6	32.7 ± 0.1	30.9 ± 1.5	25.9
Zn	0.039 ± 0.010	-	-	< 0.03	-	-
Rb	0.082 ± 0.016	-	-	0.247 ± 0.030	-	-
Hg	0.328 ± 0.036	-	-	0.684 ± 0.060	-	-
Pb	0.197 ± 0.035	-	-	0.494 ± 0.064	-	-

4. Conclusions

Investigations of biogenic ferrihydrite nanoparticles produced by bacteria *Klebsiella Oxytoca* by applying structural methods as small-angle X-ray and diffraction of synchrotron radiation, as well as ion beam analysis methods as particle-induced X-ray emission (PIXE), particle induced gamma-emission (PIGE) and Rutherford backscattering (RBS) with 3 MeV proton beam were accomplished and elemental composition of samples was determined.

Fe12 and Fe34 samples, separated from a bacterial biomass grown during 8 and 21 days, respectively, showed different crystal structure, i.e. for Fe12, a tetragonal cell model and for Fe34, a monoclinic cell, respectively, give best fits to the their diffraction spectra. At nanoscale level, small-angle X-ray scattering revealed fractal type structural features, i.e. for Fe12, a mass fractal type and for Fe34, a surface fractal type, respectively were obtained.

A total 20 elements were quantitatively determined by ion beam analysis techniques in the investigated samples. From them, 14 elements were determined by PIXE, 5 elements by PIGE and 9 elements by RBS. Common elements measured by different techniques: K and Ca by PIXE and PIGE; P, Cl and Fe by PIXE, PIGE and RBS.

Similar mass fractions for O and Al in both samples, higher contents of Fe, P, Si, C, Hg, Pb, and Rb in Fe34 (ratios between 1.2 and 3), and higher contents of H, Ca, K, Mg, N, Na, and Cl in Fe12 (ratios between 1.2 and 10) were noted. In addition, Cr and S in Fe34, and Zn and Mn in Fe12 were put in evidence.

Acknowledgements

The work was accomplished in the frame of IFIN-HH User Beam schedule at the 3 MV Tandetron accelerator and partially was supported by the Joint Institute for Nuclear Research (JINR) Dubna

Theme No. 04-4-1121-2015/2017, RO-JINR Projects Nos. 95/15.02.2016 and 96/15.02.2016, items 77, 82; Nos. 219/10.04.2017 and 220/10.04.2017 item 38; RFBR and Krasnoyarsk region Project No. 17-43-240527. Support by the Special Program for Siberian Federal University of the Ministry of Education and Science of the Russian Federation is acknowledged.

References

[1] M. Sastry, A. Ahmad, M.I. Khan, R. Kumar, Current Science 85 (2), 162 (2003).
[2] M. Balasoiu, A.I. Kuklin, G.M. Arzumanyan, T.N. Murugova, S.V. Stolyar, R.S. Iskhakov, L.A. Ishchenko, Yu.L. Raikher, Biogenic nanoparticles produced by bacteria Klebsiella oxytoca: structure investigations. In: Modern Trends in Nanoscience, Ed. Maria Balasoiu and Grigory M. Arzumanyan, The Publishing House of the Romanian Academy (Editura Academiei Române), Bucharest, 2013, pp. 179-196.
[3] A. Guinier and G. Fournet, Small-Angle Scattering of X-Rays, John Wiley & Sons, New York, Chapman & Hall, Ltd, London (1995)
[4] J.R. Tesmer, M. Nastasi, Handbook of Modern Ion Beam Materials Analysis. Materials Research Society, Pittsburg, Pennsylvania, USA (1995).
[5] S. V. Stolyar, O.A. Bayukov, D.A. Balaev, R.S. Iskhakov, L.A. Ishchenko, V.P. Ladygina, R.N. Yaroslavtsev, Journal of Optoelectronics and Advanced Materials 17 (7-8), 968-972 (2015).
[6] S. V. Stolyar, O. A. Bayukov, Yu.L. Gurevich, E.A. Denisova, R.S. Iskhakov, V.P. Ladygina, A.P. Puzyr', P.P. Pustoshilov, M.A. Bitekhtina, Inorganic Materials 42, 763 (2006).
[7] S. V. Stolyar, O. A. Bayukov, Yu. L. Gurevich, V. P. Ladygina, R.S. Iskhakov, P.P. Pustoshilov, Inorganic Materials 43, 638 (2007).
[8] Yu.L. Raikher, V.I. Stepanov, S.V. Stolyar, V.P. Ladygina, D.A. Balaev, L.A. Ishchenko, M. Balasoiu, Phys. of Solid State 52 (2) 277 (2010).
[9] M. Balasoiu, S.V. Stolyar, R.S. Iskhakov, Yu.L. Raikher, A.I. Kuklin, O.L. Orelovich, Yu.S. Kovalev, T.S. Kurkin, G.M. Arzumanian, Romanian Journal of Physics 55 (7-8), 782-789 (2010).
[10] M. Balasoiu, L.A. Ishchenko, S.V. Stolyar, R.S. Iskhakov, Yu.L. Raikher, A.I. Kuklin, D.V. Soloviov, T.S. Kurkin, D. Aranghel, G.M. Arzumanian, Optoelectronics and Advanced Materials – Rapid Communications 4 (12), 2136-2139 (2010).
[11] L.A. Ishchenko, S.V. Stolyar, V.P. Ladygina, Yu.L. Raikher, M. Balasoiu, O.A. Bayukov, R.S. Iskhakov, E.V. Inzhevatkin, Physics Procedia 9, 279-282 (2010).
[12] S.V. Stolyar, O. A. Bayukov, V.P. Ladygina, R.S. Iskhakov, L.A. Ishchenko, V.Yu. Yakovchuk, K.G. Dobretsov, A.I. Pozdnyakov, O.E. Piksina, Physics of the Solid State 53 (1), 100–104 (2011).
[13] L. Anghel, M. Balasoiu, L.A. Ishchenko, S.V. Stolyar, T.S. Kurkin, A.V. Rogachev, A.I. Kuklin, Y.S. Kovalev, Y.L. Raikher, R.S. Iskhakov, G. Duca, Journal of Physics: Conference Series 351, 012005, (2012).
[14] C.G. Chilom, D.M. Găzdaru, M. Bălăsoiu, M. Bacalum, S.V. Stolyar, A.I. Popescu, Romanian Journal of Physics 62, 701(13) (2017).
[15] V.L. Aksenov , V.P. Glazkov, S.E. Kichanov, D.K. Pogoreliy, K.M. Podurets, V.A. Somenkov, B.N. Savenko, E.V. Yakovenko, Nuclear Instruments and Methods in Physics Research A 575, 266–268 (2007).
[16] https://tandem.nipne.ro/accelerators.php
[17] G. Beaucage, J. Appl. Cryst. 29, 134-146 (1996).
[18] A.Yu. Cherny, E.M. Anitas, A.I. Kuklin, M. Balasoiu and V. A. Osipov, J. Appl. Cryst. 43, 790–797 (2010).
[19] A.Yu. Cherny, E. M. Anitas, V.A. Osipov and A.I. Kuklin, J. Appl. Cryst. 47, 198-206 (2014).
[20] S. Kichanov, A. Pantelica, D. Pantelica, S. Stolyar, R. Iskhakov, D. Aranghel, P. Ionescu, R. Vladoiu, M. Balasoiu, Romanian Reports in Physics, 70 (2018) (in press).